Spin-dependent observables in electron-sodium scattering calculated using the coupled-channel optical method

Igor Bray* and Ian E. McCarthy†

Electronic Structure of Materials Centre, School of Physical Sciences, The Flinders University of South Australia, G.P.O. Box 2100, Adelaide 5001, Australia

(Received 5 June 1992)

We present coupled-channel optical (CCO) calculations of the elastic and the $3\,^2S$–$3\,^2P$ transitions in electron-sodium scattering at 1 to 40 eV. The results are compared with the measurements of spin asymmetries A_{ex}, the ratio of final- to initial-spin polarization perpendicular to the scattering plane P'/P, and the angular momentum transferred to the atom perpendicular to the scattering plane for singlet $L_\perp^S$, triplet $L_\perp^T$, and spin-averaged $L_\perp$. We find excellent agreement with measurements of all of these parameters at all energies. For energies above the ionization threshold we find that inclusion of the continuum target states in the CCO formalism has a very large effect on the spin asymmetries, particularly the $3\,^2P$ channel, and brings about excellent agreement with experiment. The treatment of the dynamics of the interaction is such that the quality of the structure approximation of the sodium atom may be readily studied.

PACS number(s): 34.80.Bm, 34.80.Dp, 34.80.Nz

I. INTRODUCTION

In order to obtain a thorough test of any general electron-atom scattering theory it is necessary to have an extensive set of reliable measurements of various observables at many energies and angles. From the theoretical point of view two aspects of the scattering theory require testing. First we must be able to describe the structure of the atom, together with the complete set of excited target states, in the absence of the projectile. Second we must be able to take into account the dynamics of the interaction correctly. One of the more difficult aspects of the dynamics is the proper treatment of the exchange between the projectile electron and the atomic electrons. Another problem involves incorporating the effect of the infinite set of discrete target excited states as well as the target continuum.

Rather than testing the descriptions of the structure and the dynamics simultaneously, an electron-atom scattering theory may first be applied to the hydrogen atom. This system is ideal for the theorist as the atomic structure is simple and is known analytically. A great deal of theoretical attention has been given to electron-hydrogen scattering. Unfortunately atomic hydrogen is a very difficult target for experimentalists. Though there is a great deal of data at a very broad range of energies, most data are averaged over the singlet and triplet spin states, thus losing the information that allows a direct test of the theoretical treatment of exchange.

A most extensive set of measurements that select spin states has been carried out for electron scattering on sodium by McClelland, Kelley, and Celotta [1, 2], Scholten *et al.* [3], Kelley *et al.* [4], and Lorentz *et al.* [5]. They measured the ratio of triplet-to-singlet scattering for the $3\,^2S$–$3\,^2S$ and $3\,^2P$–$3\,^2S$ channels, as well as the angular momentum transferred to the atom perpendicular to the scattering plane for singlet, triplet, and spin-averaged scattering. The inelastic data were gathered using superelastic techniques. We use the fact that the theory is time-reversal independent, i.e., the $3\,^2S$–$3\,^2P$ channel is equivalent to the $3\,^2P$–$3\,^2S$ channel. In addition there are the measurements of the ratio of final-to-initial polarization perpendicular to the scattering plane carried out by Hegemann *et al.* [6]. All of these measurements involve the determination of ratios at each angle, which do not suffer from the considerable difficulties associated with accurate measurements necessary in absolute experiments, such as when measuring differential cross sections.

Whilst the structure of the sodium atom is not as simple as that of hydrogen it is very well modeled as a hydrogenlike atom of one valence electron above a frozen core. Zhou *et al.* [7] showed that the frozen-core one-electron wave functions of the sodium atom can be improved by the addition of a phenomenological polarization potential which leads to eigenenergies which are in excellent agreement with experiment.

The electron-atom scattering theory that we use is the coupled-channel optical (CCO) method based on the work of McCarthy and Stelbovics [8]. This is a generalization of the close-coupling (CC) formalism where only a finite set of the low-lying target discrete states are coupled together. In the CCO method we also couple the low-lying target discrete states (P space), but in addition the effect of the higher discrete and continuum states (Q space) is taken into account via a complex nonlocal polarization potential. This potential is calculated *ab initio* in the weak-coupling approximation [9]. By this we mean that we do not allow any coupling between distinct Q-space states, but direct coupling between P-space states and Q-space states is included. This approximation is readily tested for discrete states by seeing the effect of in-

terchanging a particular state between P and Q spaces. The only way we have of testing the treatment of the continuum is by comparison with experiment.

Our CCO formalism using symmetric P and Q projection operators [9] has been extensively tested at a broad range of energies by getting excellent agreement with differential cross-section measurements of electron scattering on atomic hydrogen [9, 10] and on sodium [11, 12]. The theory is applicable to the complete energy range spanning the low-, intermediate-, and high-energy regions of atomic physics.

In a preliminary report of this work [13] we showed that the spin asymmetries at 10 and 20 eV are greatly influenced by continuum states. We found that at some angles the inclusion of the continuum leads to a large change from singlet dominance to triplet dominance, and is in complete agreement with experiment. This confirms an earlier finding of McCarthy, Mitroy, and Nicholson [14], who approximated the optical potential by an equivalent local potential. In this work we apply our CCO theory to the broad range of energies measured by McClelland and co-workers [1–5]. We find that the quality of the scattering theory is so good (general quantitative agreement with experiment is achieved at all energies) that we are able to examine the quality of the structure representation as well.

II. THEORY

Before we can begin writing down the CCO equations of scattering we must define the approximations we use in describing the structure of the sodium atom. We get the one-electron core wave function $|\psi_j\rangle$ by solving the self-consistent-field Hartree-Fock equations [15] for the ground state of the sodium atom. As in Refs. [11, 12] to get the complete set of one-electron noncore target states $|\phi_j\rangle$, discrete and continuous orthogonalized to the core states, we solve the frozen-core Hartree-Fock equations [16]. However, we also add a phenomenological core-polarization potential, which considerably improves the one-electron energies. Calculations that use wave functions generated with this potential we denote by FCHF$^+$, and those without by FCHF. Thus our noncore target states $|\phi_j\rangle$ satisfy

$$\left(K + v^{\mathrm{FC}} - \epsilon_j\right)\phi_j(\mathbf{r}) = 0, \qquad j \notin C \tag{1}$$

where

$$v^{\mathrm{FC}}\phi_j(\mathbf{r}) = \left(-\frac{Z}{r} + v_{\mathrm{pol}}(r) + 2\sum_{\psi_{j'}\in C}\int d^3r' \frac{|\,\psi_{j'}(\mathbf{r}')\,|^2}{|\,\mathbf{r}-\mathbf{r}'\,|}\right)\phi_j(\mathbf{r}) - \sum_{\psi_{j'}\in C}\int d^3r' \frac{\psi^*_{j'}(\mathbf{r}')\phi_j(\mathbf{r}')}{|\,\mathbf{r}-\mathbf{r}'\,|}\psi_{j'}(\mathbf{r}), \tag{2}$$

and where the notation C indicates the set of frozen-core states. For sodium we take the core to be $1s^22s^22p^6\ {}^1S$. The polarization potential v_{pol}, which is intended to approximate virtual excitations of the core, is given by Zhou *et al.* [7]

$$v_{\mathrm{pol}}(r) = \frac{-\alpha_d}{2r^4}\{1 - \exp\left[-(r/\rho)^6\right]\}, \tag{3}$$

where $\alpha_d = 0.99a_0^3$ and $\rho = 1.439a_0$. With this choice of the polarization potential we reproduce the experimental ionization energies [17] to almost four significant figures, an improvement of around two significant figures on the plain frozen-core model, see Table I. In our earlier work [11–13] we believed that having correct one-electron energies and associated wave functions $|\phi_j\rangle$ was not very important away from excitation thresholds. In the course of the present work we found that these play a small, but significant, role in the description of the $L_\perp$ parameter at all energies.

The theory that we use to describe electron-atom scattering is based on the work of McCarthy and Stelbovics [8]. They formed and showed how to solve the CCO equations in momentum space using the Lippmann-Schwinger equation. The major enhancements have been carried out by Bray, Konovalov, and McCarthy [9] who defined a considerably improved optical potential using symmetric P and Q projection operators, and Bray *et al.* [18] who showed how to solve the coupled equations using the distorted-wave representation. The latter is a computational technique used throughout this work which considerably reduces the numerical difficulties associated with solving the Lippmann-Schwinger equation.

Rather than treat the sodium target by the independent-particle model as was done in Ref. [8], we consider the electron-sodium scattering system as a three-body problem of an inert core, one valence, and one projectile electron. The problem is then similar to the electron-hydrogen scattering problem, except that the local electron-proton potential is replaced by the nonlocal electron-core potential v^{FC} of Eq. (2).

All matrix elements in the Lippmann-Schwinger equation are written as two-electron matrix elements. This integral equation for the T^S matrix, where S is the total spin, in the distorted-wave representation [18] is

$$\langle \mathbf{k}^{(-)}\phi_i \mid T^S \mid \phi_0\mathbf{k}_0^{(+)}\rangle = \langle \mathbf{k}^{(-)}\phi_i \mid V_Q^S(\theta) \mid \phi_0\mathbf{k}_0^{(+)}\rangle + \sum_{\phi_{i'}\in P}\int_{\mathbf{k}'} \frac{\langle \mathbf{k}^{(-)}\phi_i \mid V_Q^S(\theta) \mid \phi_{i'}\mathbf{k}'^{(-)}\rangle}{(E^{(+)} - \epsilon_{i'} - k'^2/2)}\langle \mathbf{k}'^{(-)}\phi_{i'} \mid T^S \mid \phi_0\mathbf{k}_0^{(+)}\rangle, \tag{4}$$

TABLE I. Ionization energies (eV) of the low-lying sodium states. The pure frozen-core Hartree-Fock results are denoted by FCHF. The results with an added phenomenological polarization potential given in Eq. (3) are denoted by FCHF$^+$. The experimental values are due to Moore [17].

State	FCHF	FCHF$^+$	Expt.
$3s$	4.956	5.140	5.139
$4s$	1.910	1.947	1.948
$5s$	1.009	1.022	1.024
$6s$	0.622	0.629	0.630
$3p$	2.980	3.040	3.038
$4p$	1.370	1.387	1.387
$5p$	0.787	0.795	0.795
$6p$	0.511	0.515	0.516
$3d$	1.515	1.522	1.523
$4d$	0.852	0.856	0.856
$5d$	0.545	0.547	0.548
$6d$	0.379	0.380	0.381
$4f$	0.850	0.851	0.851
$5f$	0.544	0.544	0.545
$6f$	0.378	0.378	0.379

where the projectile with momentum $\mathbf{k}_0$ is incident on the target with the valence electron in the ground state $|\phi_0\rangle$, energy ϵ_0, above the frozen core, and where $E = \epsilon_0 + k_0^2/2$ is the on-shell energy. The indices $(+)$ or $(-)$ are used to indicate outgoing or incoming spherical-wave boundary conditions, respectively. The distorted waves $|\mathbf{k}^{(\pm)}\rangle$ are the complete set of solutions (including bound states) of

$$(K+U)|\mathbf{k}^{(\pm)}\rangle = \varepsilon_k|\mathbf{k}^{(\pm)}\rangle, \tag{5}$$

where we take U to be

$$U(r) = -\frac{Z}{r} + v_{\rm pol}(r) + 2\sum_{\psi_{j'}\in C}\int d^3r' \frac{|\,\psi_{j'}(\mathbf{r}')\,|^2}{|\,\mathbf{r}-\mathbf{r}'\,|} + \int d^3r' \frac{|\phi_0(\mathbf{r}')|^2}{|\,\mathbf{r}-\mathbf{r}'\,|}. \tag{6}$$

The most important criterion that this potential satisfies is that it is $-Z/r$ at the origin, and falls to zero quite rapidly. This potential is used to remove the $-Z/r$ behavior at the origin in the $V_Q^S(\theta)$ matrix elements in (4), and so achieves very rapid convergence in the integrand as a function of increasing k'. Utilizing the potential U, the maximum k' that we require in (4) is of order 3 a.u., whereas without it we require k' of order 100 a.u.. This potential is very useful in testing the numerical analysis since the solution of the Lippmann-Schwinger equation (4) must be independent of U.

Writing the coordinate space-exchange operator as P_r the matrix elements of $V_Q^S(\theta)$ are given [9, 18, 19] by

$$\langle \mathbf{k}\phi_i \mid V_Q^S \mid \phi_{i'}\mathbf{k}'\rangle = \langle \mathbf{k}\phi_i \mid v^{\rm FC} - U + v_{12}(1+(-1)^S P_r) \mid \phi_{i'}\mathbf{k}'\rangle + (-1)^S(1-\theta)(\epsilon_i+\epsilon_{i'}-E)\langle \mathbf{k}|\phi_{i'}\rangle\langle\phi_i|\mathbf{k}'\rangle + \delta_{ii'}\theta\sum_{\phi_n\in P}(\epsilon_i+\epsilon_n-E)\langle \mathbf{k}|\phi_n\rangle\langle\phi_n|\mathbf{k}'\rangle + \langle \mathbf{k}\phi_i \mid V_Q + (-1)^S V_Q P_r \mid \phi_{i'}\mathbf{k}'\rangle, \tag{7}$$

where v_{12} is the electron-electron potential, and V_Q is the complex nonlocal polarization potential [9] which is calculated *ab initio* subject to the weak-coupling approximation in Q space. The constant θ above is arbitrary. Bray and Stelbovics [19] have shown that any nonzero θ leads to a unique answer for the T matrix independent of θ, both on and off the energy shell. In our previous work [9–12] we had in effect $\theta = 0$. Stelbovics [20] has shown that for $\theta = 0$ only the on-shell T matrix is defined uniquely which explains why we achieved stable results. However, we have found that as the number of P-space states is increased, off-shell instability affects the on-shell stability. This problem is eliminated for $\theta \neq 0$. In this work we take $\theta = 1$ since it completely eliminates the second term in (7).

Another major difference in the potential matrix elements used here is the absence of core-overlap exchange terms (see Refs. [12, 13] for example) that arose when McCarthy and Stelbovics [8] treated alkali-metal atoms by the independent-particle model. We found that these terms do not make any notable contribution, validating the treatment of the sodium-electron scattering system as a three-body problem.

The Lippmann-Schwinger equation (4) is solved in partial-wave formalism [8] with each partial wave being treated in exactly the same way, with as many partial waves taken as necessary for convergence. We take advantage of the fact that for nonelastic channels for sufficiently large total orbital angular momentum the T matrix approaches the first Born matrix element, and we are able to take account of the higher partial waves by doing an analytic Born subtraction [8] without having to calculate them. For the elastic channel, large partial-wave matrix elements are dominated by the dipole polarization, which is not included in the Born approximation. We extrapolate, if necessary, using the relation [21] $T \approx \alpha/L^3$, where α is derived by matching. The number of partial waves that we calculate varies with the projectile energy. For example at 1, 10, and 40 eV we calculate, respectively, 10, 30, and 60 partial waves explicitly by solving the Lippmann-Schwinger equation.

The relations between various observables, such as the spin asymmetry $A_{\rm ex}$ or $L_\perp$, and the partial T-matrix elements may be found in Ref. [10]. Writing the direct and exchange amplitudes as f and g, respectively, with corresponding singlet $S = f + g$ and triplet $T = f - g$ amplitudes, the ratio of the final-to-initial polarization perpendicular to the scattering plane P'/P is given by [6]

$$P'/P = 1 - |g|^2/\sigma, \tag{8}$$

where $\sigma = (|S|^2 + 3|T|^2)/4$ is the differential cross section. This ratio has been measured for electron-sodium scattering at 4.0 and 12.1 eV by Hegemann *et al.* [6]. For the elastic channel, writing $S = a_s e^{i\gamma_s}$ and $T = a_t e^{i\gamma_t}$, McClelland *et al.* [2] expressed P'/P as

$$P'/P = \frac{2r + 2\sqrt{r}\cos(\pm\gamma_{st})}{1+3r}, \quad \gamma_{st} = \gamma_s - \gamma_t \tag{9}$$

where $r = |T|^2/|S|^2$ is the ratio of triplet-to-singlet scattering, and combined their measurements of r with those of P'/P to provide a set of measurements for $\cos\gamma_{st}$. This gives a measured value for the magnitude of γ_{st}.

The ratio r may be equivalently expressed as spin asymmetry $A_{\rm ex}$,

$$A_{\rm ex} = \frac{1-r}{1+3r}. \tag{10}$$

The spin asymmetry $A_{\rm ex}$ has the advantage that it always remains finite with a minimum of $-1/3$ when triplet scattering is dominant (r is infinite), and a maximum of 1 when singlet scattering is dominant ($r = 0$). A value of zero indicates that $|S|^2 = |T|^2$, which often indicates that the exchange amplitude is zero.

The determination of $A_{\rm ex}$ or r, the absolute differential cross section, and the phase difference γ_{st} completes the characterization of the elastic-scattering process. For the inelastic-scattering process $3\,^2S$–$3\,^2P$, or its time reversal, the situation is a little more complicated. Here the singlet and triplet amplitudes split into two parts, one for each magnetic sublevel $M_L = +1$ and $M_L = -1$ (the "natural" coordinate system is being used, i.e., the z axis is normal to the scattering plane). Experimentally, the magnitudes of these four amplitudes S_{+1}, S_{-1}, T_{+1}, and T_{-1} may be determined by measuring the differential cross section, the ratio of triplet-to-singlet scattering, both summed over the magnetic sublevels, as well as the angular momentum transferred to the atom perpendicular to the scattering plane [4] for singlet

$$L_\perp^S = \frac{|S_{+1}|^2 - |S_{-1}|^2}{|S_{+1}|^2 + |S_{-1}|^2} \tag{11}$$

and triplet

$$L_\perp^T = \frac{|T_{+1}|^2 - |T_{-1}|^2}{|T_{+1}|^2 + |T_{-1}|^2} \tag{12}$$

scattering. The spin-averaged $L_\perp$ is

$$L_\perp = \frac{|S_{+1}|^2 - |S_{-1}|^2 + 3(|T_{+1}|^2 - |T_{-1}|^2)}{|S_{+1}|^2 + |S_{-1}|^2 + 3(|T_{+1}|^2 + |T_{-1}|^2)}. \tag{13}$$

III. DISCUSSION

Before we proceed to do any calculations we have to decide which discrete target states to include in P space. The matrix elements of the operator V_Q are calculated in the approximation that neglects coupling between distinct Q-space states. This approximation is readily tested internally for the discrete Q-space states. In calculating differential cross sections [11,12] we found that it is a very good approximation. Its main advantage is that it allows a relatively small number of P-space states to be used, which saves considerable computational time. In testing this approximation, when calculating the spin asymmetry and $L_\perp$ parameters, we found that it was not as good as it was for the differential cross sections. This can be seen in the work by Madison, Bartschat, and McEachran [22] who compared experiment and their distorted-wave second-order-Born (DWB2) calculations with the 3CCO [12] spin asymmetries and $L_\perp$ generated from the T-matrix elements that were only checked against stability in the differential cross sections.

The remedy is very simple. As it is the calculation of the continuum contributions that takes around 95% of the computational time, we first take as large a P space as necessary to get complete convergence in the treatment of the discrete states. We then add the continuum contributions to as many of the low-lying P-space states as necessary, until convergence has been obtained.

We find this approach rather attractive. Using techniques outlined by Bray and Stelbovics for real potentials [19] we can find the number of discrete states necessary for complete convergence just using the close-coupling formalism very quickly. Having found the minimal P space necessary for convergence we proceed to add the contributions from the complex polarization potential V_Q for the continuum to the potential matrix elements coupling the low-lying states of P space. This allows us to observe the effect of the continuum on the scattering as well as observing the convergence as the number of P-space states with continuum contributions is increased. We denote such calculations by the notation nCCOm, where we use n to denote the number of P space states, and m the number of states whose coupling has continuum contributions. It is the magnitude of m that dominates the length of the calculation. Previously, as in [12], for example, we used the notation mCCO to indicate that there were m P-space states and each one had a contribution from Q space. A calculation nCCOm with $n \geq m \geq 1$ takes approximately the same amount of computational time as the corresponding mCCO calculation, and the former has the advantage of treating the n P-space discrete states without resorting to the weak-coupling approximation for any of the discrete states. In this formalism Q space contains only the continuum. However, not all couplings between P-space states and the continuum have been included. In particular, by computational necessity the couplings between the high-lying P-space states and the continuum are omitted. These couplings were also never included in the mCCO calculations. Another advantage of the nCCOm calculations over the mCCO ones is that the transitions between the ground state and all of the n elastic and excited states are simultaneously calculated.

The number of P-space states necessary for complete convergence depends on the scattering channel of interest and the projectile energy. In this work we concentrate on the elastic and $3\,^2P$ channels. We found that of the energies which we considered the one requiring the largest number of P-space states was 4.1 eV. These states were the 15 states that have the principal quantum number

range from 3 to 6 and orbital angular-momentum range from 0 to 3 (see Table I for the one-electron energies). To get convergence in the inclusion of continuum contributions we had to have these contributions in the first six states with $l \leq 2$. We denote these calculations by 15CCO6, each of which takes approximately 2 h CPU time per partial wave on our local IBM RS6000/530 computers. A corresponding 15CC calculation takes only 6 min per partial wave. The reason that the continuum contributions take so long is that the nonlocal complex polarization potential V_Q is a second-order term which is generated for each channel by incorporating over 100 continuum states (20 states for each $l = 0$ to 5) used to integrate over the continuum momentum [9].

IV. RESULTS

We apply our CCO theory at projectile energies where there is a considerable set of measurements of spin-dependent observables. The results are presented only in pictorial form. The spin-dependent complex amplitudes at 1° intervals for the transition from the ground state to any one of the 15 states in Table I, or results at a different energy to those presented here, may be obtained by sending an electronic-mail request to the first author.

In Fig. 1 we look at the elastic spin asymmetries measured by Lorentz *et al.* [5] at projectile energies of 1.0 and 1.6 eV. At these very low energies, below the first excitation threshold of 2.1 eV for the $3\,^2P$ channel (see Table I), only the virtual excitation of the first few low-lying excited states is necessary to achieve convergence to better than 5%. The effect of the continuum is completely negligible. We compare two 15CC calculations with experiment. One, which we denote by FCHF$^+$, uses the phenomenological polarization potential (3) to define the noncore wave functions. The other, denoted by FCHF, leaves this potential out. We see that at 1.0 eV the two calculations are not very different, and are in good agreement with experiment. However, at 1.6 eV there is a very large discrepancy between the two calculations with the FCHF$^+$ being in excellent agreement with experiment. It should be noted that we do not expect perfect quantitative agreement at these energies. Apart from the fact that we are treating electron-sodium scattering as a three-body problem, the electron beam used in the experiment has a width of around 0.1 eV. Our investigations have shown that the rate of change in the asymmetries as a function of energy is particularly high at 1.6 eV. The differences between the FCHF$^+$ and FCHF calculations are indicative of this rate of change. At all other energies, unless otherwise stated, we use the FCHF$^+$ model for the wave functions.

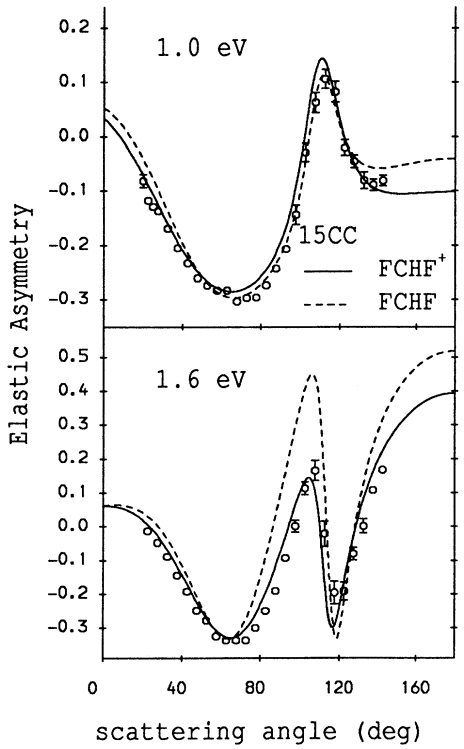

FIG. 1. Elastic spin asymmetries calculated using 15-state close-coupling for electron-sodium scattering at projectile energies of 1.0 and 1.6 eV. The calculation denoted FCHF$^+$ uses the phenomenological polarization potential (3) to improve the electron ionization energies, FCHF does not. The measurements are due to Lorentz *et al.* [5]. Quantitative results may be obtained by corresponding with the first author.

In Fig. 2 we compare the results of our 15CCO6 and 15CC (to see the effect of the continuum) calculations at 4.1 eV, with various measured observables. The measurements of P'/P (Hegemann *et al.* [6]) were performed at 4.0 eV; however, we found that the theoretical results are not significantly altered between these two energies, and we presume that this is the case experimentally also. Whilst there is a discrepancy at the backward angles for this and the derived $\cos\gamma_{st}$ parameter, we are informed [23] that at this energy the effect of sodium dimer molecules may be to increase the P'/P measurements by up to 0.06 at backward angles. This may be the cause of this discrepancy.

At this energy the ionization channel is still closed, so as expected the effect of the continuum on the scattering is very small. We find very good agreement with the spin asymmetries (McClelland *et al.* [1,2]) for both channels and with the $L_\perp$ parameters. For the $3\,^2P$ channel we present the equivalent spin asymmetry and the ratio measurements to show how they are related.

In Fig. 3 we compare the 15CCO6, 15CC, and the DWB2 of Madison, Bartshat, and McEachran [22] calculations at 10 eV with various measured observables. At this energy the complete set of excited discrete and ionization channels is open. We see that whilst the 15CC calculation, which is convergent in the treatment of the discrete states, gets good qualitative agreement with experiment (Scholten *et al.* [3], Kelley *et al.* [4]) the addition of the continuum contributions brings about excellent quantitative agreement with the exception of the singlet $L_\perp$ parameter near 60°. We will see that this problem is unique only to this energy. At all other energies we require only small contributions from the continuum to any of the $L_\perp$ parameters in order to get quantitative agreement with experiment. This may prove to be a test

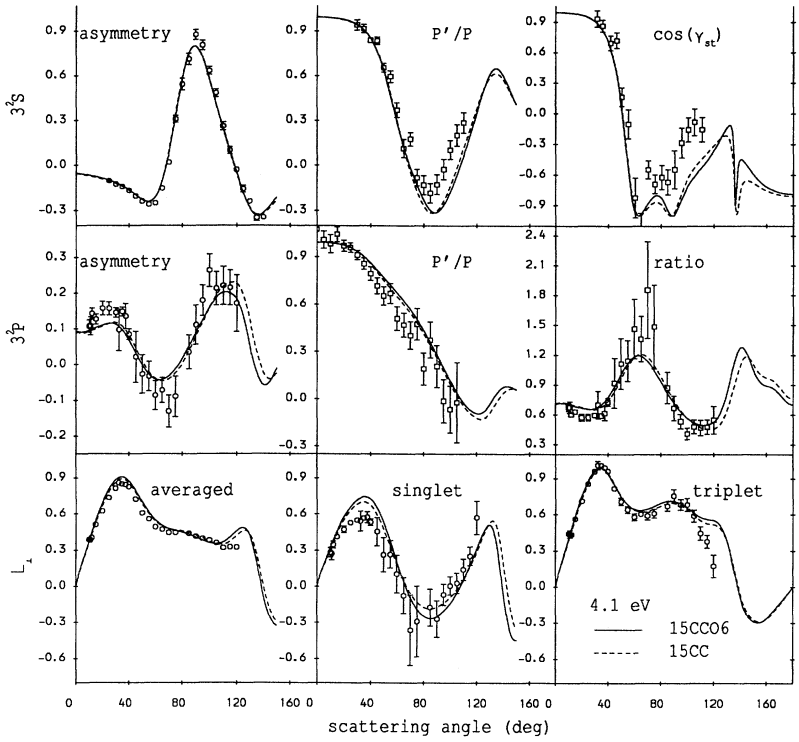

FIG. 2. Calculations of spin-dependent observables for electron-sodium scattering at projectile energy of 4.1 eV. The calculation denoted by 15CCO6 has the effect of the continuum added to the first six states of the 15CC calculation. The P'/P measurements (at 4.0 eV) are due to Hegemann *et al.* [6]. The rest are due to McClelland *et al.* [1, 2]. Quantitative results may be obtained by corresponding with the first author.

case for an exact treatment of the effect of the continuum on the scattering. It is interesting to note also that the measurements of the ratio r and the $L_\perp$ parameters are not independent. For example,

$$L_\perp^S = L_\perp + 3r(L_\perp - L_\perp^T). \tag{14}$$

This relation holds for the measurements presented, and naturally for the theory as well. Though we get apparently good agreement with all the parameters on the right-hand side of the above equation, this turns out to be deceptive when we compare the combined results. This emphasizes the importance of having measurements of

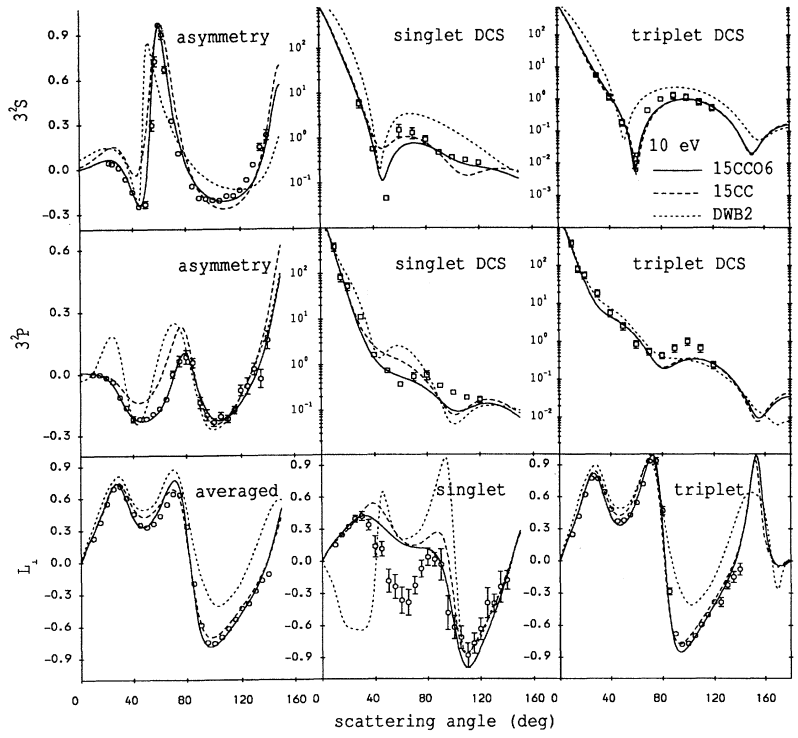

FIG. 3. Calculations of spin-dependent observables for electron-sodium scattering at projectile energy of 10 eV. The calculation denoted by 15CCO6 has the effect of the continuum added to the first six states of the 15CC calculation. The second-order distorted-wave Born calculation of Madison, Bartschat, and McEachran [22] is denoted by DWB2. The measurements denoted by ○ are due to Scholten *et al.* [3] (inelastic) and Kelley *et al.* [4] (elastic). The measurements denoted by □ are a combination of the measurements of the differential cross section by Srivastava and Vušković [24] and the spin asymmetries. Quantitative results may be obtained by corresponding with the first author.

spin-dependent observables for a thorough test of theory.

We followed the example of McClelland *et al.* [2] to generate the differential cross section for both singlet and triplet scattering by combining the measurements for the spin asymmetry with those of the spin-averaged differential cross section (Srivastava and Vušković [24]). These are in good quantitative agreement with our results.

The DWB2 calculation is surprisingly good at this energy. As it is based on a perturbative approach we do not expect it to be convergent at this low energy. It will be interesting to see how the DWB2 calculation improves further with increasing energy.

In the next figure (Fig. 4) we compare various measurements at 12.1 eV with the 15CCO6 and 15CC calculations. The latter is calculated with two sets of wavefunctions $FCHF^+$ and FCHF. We do this to show what effect the choice of wave functions has on the scattering at an energy well away from any excitation threshold. We see that there is an angular shift to the left from the $FCHF^+$ to the FCHF calculations in the $L_\perp$ parameters, most pronounced for the triplet and summed $L_\perp$. This happens to be the situation at the other energies also (see Bray [13] for calculations of $L_\perp^S$ and $L_\perp^T$ at 10 and 20 eV using FCHF wave functions). Since in the triplet and spin-averaged cases there is a very large rate of change in the intermediate angular range, we find that the $FCHF^+$ calculations result in much better agreement with experiment than the corresponding FCHF calculations.

By comparing the 15CCO6 with the 15CC results we once again see that the effect of the continuum is quite large and brings about excellent agreement with experiment. At this energy we can claim complete quantitative agreement with available measurements of the spin asymmetry and $\cos\gamma_{st}$ (McClelland *et al.* [2]), P'/P (Hegemann *et al.* [6]), and $L_\perp$ (Scholten *et al.* [25])]. It is unfortunate that spin-resolved measurements of the latter parameter are not available at this energy, and so we are unable to see if the discrepancy at 10 eV for the $L_\perp^S$ is also a problem at 12.1 eV. Given the demonstrated sensitivity of the $L_\perp^S$ parameter at 10 eV, it is worth noting that agreement around 60° with the spin-averaged $L_\perp$ at this energy is considerably better than at 10 eV.

As at 4.1 eV, we give both the spin asymmetry and the ratio for the $3\,^2P$ channel. In this case the effect of the continuum is greatly emphasized at the forward angles by looking at the ratio parameter.

In Fig. 5 we look at the 20-eV results. Here we see the greatest effect of the continuum on the spin asymmetries (McClelland *et al.* [1], Kelley *et al.* [4]), which brings about remarkable agreement with experiment. For the inelastic channel, while qualitative agreement is excellent, quantitative agreement is not as good as it was at 10 eV where the effect of the continuum was smaller. Agreement with the $L_\perp$ parameters is complete, with the continuum having only a marginal effect. This underlines the sensitivity of the asymmetry parameter. Using the relation (14) we can express r, and therefore A_{ex}, in terms of just the $L_\perp$ parameters. Looking at 120°, for example, we see excellent agreement between experiment and theory for the $L_\perp$ parameters. However, agreement between theory and experiment for the A_{ex} parameter at this angle is quite poor though both theory and experiment do satisfy relation (14). Another way of seeing this sensitivity is by observing that the continuum does not

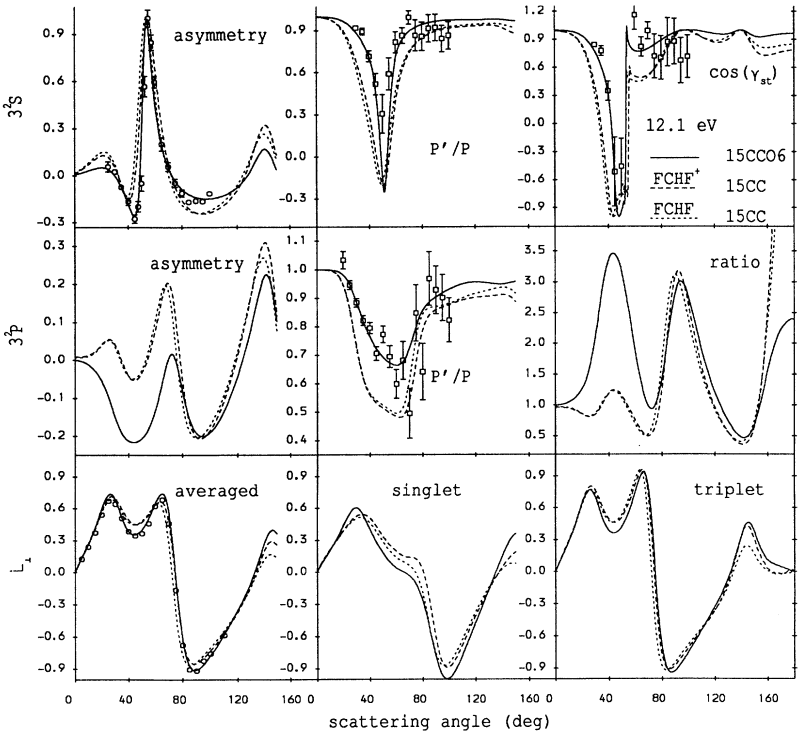

FIG. 4. Calculations of spin-dependent observables for electron-sodium scattering at projectile energy of 12.1 eV. The calculation denoted by 15CCO6 has the effect of the continuum added to the first six states of the $FCHF^+$ 15CC calculation. This calculation uses the phenomenological polarization potential (3) when calculating the noncore states of sodium whereas the FCHF calculation does not. The P'/P measurements are due to Hegemann *et al.* [6]. The measurements of the elastic asymmetry are due to McClelland *et al.* [2], and were used to generate the $\cos\gamma_{st}$ data from the P'/P measurements. The $L_\perp$ measurements are due to Scholten, Teubner, and Shen [25]. Quantitative results may be obtained by corresponding with the first author.

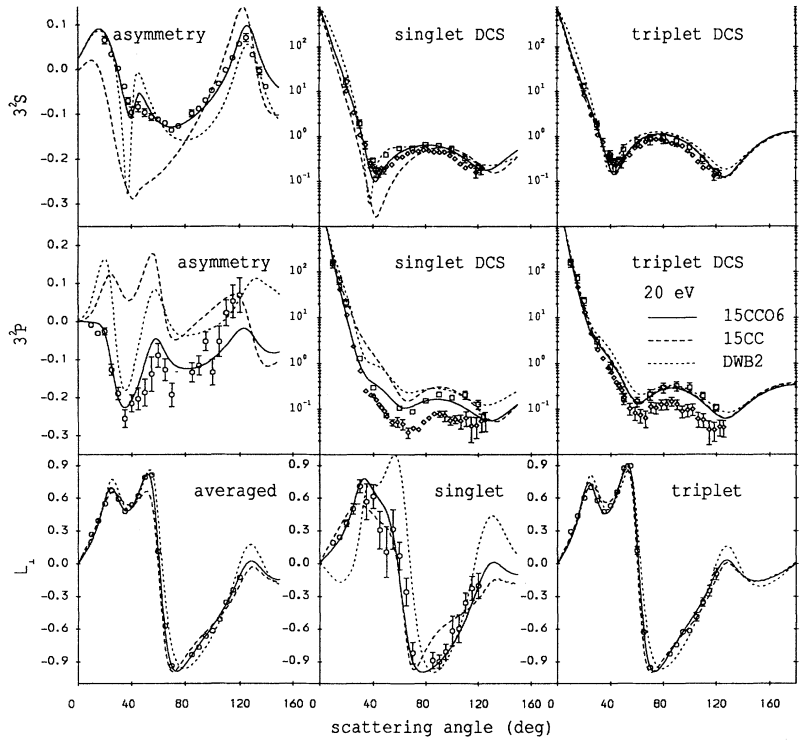

FIG. 5. Calculations of spin-dependent observables for electron-sodium scattering at projectile energy of 20 eV. The calculation denoted by 15CCO6 has the effect of the continuum added to the first six states of the 15CC calculation. The second-order distorted-wave Born calculation of Madison, Bartschat, and McEachran [22] is denoted by DWB2. The measurements denoted by ○ are due to McClelland *et al.* [1] (inelastic) and Kelley *et al.* [4] (elastic). The measurements denoted by □ and ◇ are a combination of the spin asymmetries with the measurements of the differential cross section by Srivastava and Vušković [24] and Lorentz and Miller [26], respectively. Quantitative results may be obtained by corresponding with the first author.

appear to have a large effect on the $L_\perp$ parameters, but does have a large effect on A_{ex} or r.

It is interesting to note the marked improvement in the DWB2 calculation. In fact it gets a better qualitative agreement with experiment for the asymmetries than the 15CC calculation, which is nonperturbative and treats the discrete excited states to convergence. We believe the reason for this to be due to the fact that DWB2 has the effect of the continuum in the second order whereas 15CC has no such effects.

We use the spin-unresolved measurements of the differential cross sections by Srivastava and Vušković [24] and

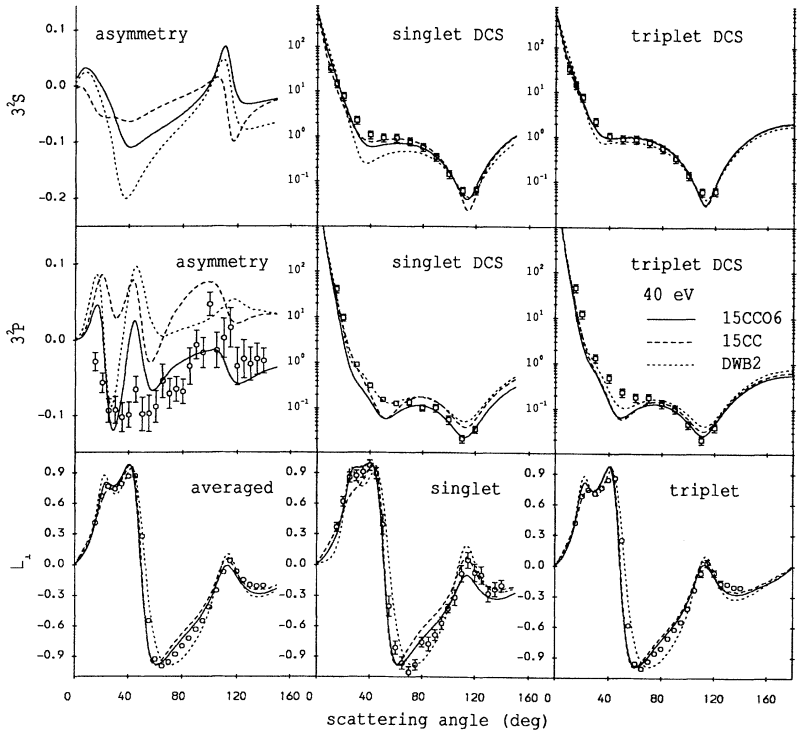

FIG. 6. Calculations of spin-dependent observables for electron-sodium scattering at projectile energy of 40 eV. The calculation denoted by 15CCO6 has the effect of the continuum added to the first six states of the 15CC calculation. The second-order distorted-wave Born calculation of Madison, Bartschat, and McEachran [22] is denoted by DWB2. The measurements denoted by ○ are due to Scholten *et al.* [3]. The measurements denoted by □ are a combination of the spin asymmetries (theoretical for elastic) with the measurements of the differential cross section by Srivastava and Vušković [24]. Quantitative results may be obtained by corresponding with the first author.

Lorentz and Miller [26] in conjunction with the asymmetry measurements to generate the singlet and triplet differential cross sections. These have been normalized to the theory using integrated cross sections, and are in good agreement with the theory.

Finally, in Fig. 6 we look at the 40-eV results. There are no elastic asymmetry measurements so we use the theoretical values to generate the singlet and triplet differential cross sections from the spin-unresolved measurements (Srivastava and Vušković [24]). We find good agreement between the measured and calculated differential cross sections.

The continuum once again has a big effect on the asymmetries for both channels. The theory predicts a bigger peak around 40° for the inelastic channel than the experiment (Scholten *et al.* [3]). This is likely to be due to the inexact treatment of the continuum. It should be noted that at this energy the magnitude of the asymmetries has dropped considerably to be much nearer zero, indicating that exchange effects are much less important at this and higher energies.

Agreement between the 15CCO6 results and the measurements of $L_\perp$ (Scholten *et al.* [3]) is excellent. The quality of the DWB2 calculation has improved markedly, particularly for the singlet $L_\perp$ parameter.

V. CONCLUSIONS

We have found that our CCO description of the reaction mechanism in electron-sodium scattering is extremely good. As a result, we have been able to test the description of the structure of the atom. Calculating the target-wave functions, with or without the phenomenological polarization potential (3), has a small but significant effect on the results. The addition of this potential considerably improves agreement of the theory at just below the first excitation threshold. This effect we anticipated. However, we also found that it shifts the $L_\perp$ parameters a few degrees to the right around the intermediate angles at all energies, thus giving excellent agreement with experiment.

By looking at the measurements of the spin asymmetries and P'/P we have seen that exchange plays a significant role (whenever $A_{\rm ex} \neq 0$, $P'/P < 1$) at all of the energies considered. For energies above the ionization threshold we saw that a close-coupling calculation that treats all bound excited states to convergence is unable to reproduce the experiment. Addition of the continuum contributions yields remarkable quantitative agreement with experiment, suggesting that the exchange amplitudes are sometimes influenced predominantly by the continuum channel.

The effect of the continuum on the $L_\perp$ parameters has been found to be relatively small at all energies, but is generally necessary to give quantitative agreement with experiment. However, the 10-eV singlet $L_\perp$ measurements suggest that at this energy the continuum should have a large effect around 60°. We conclude this because the 15CC calculation presented is convergent in the treatment of the discrete excited states. We have also checked that this region is not significantly affected by either choice of target-wave functions.

While we have presented results which give generally excellent quantitative agreement with experiment, it must be remembered that the contribution of the continuum upon the scattering has been calculated within the weak-coupling approximation. Bray and Stelbovics [19] have demonstrated that the electron-hydrogen scattering problem can be solved to convergence using very large orthogonal Laguerre-basis expansions for the target wave functions. As these result in square-integrable states, a close-coupling formalism may be applied directly without resorting to the coupled-channel optical method presented here. We intend to apply these ideas to the sodium target as well. Perhaps this will help to resolve the remaining minor discrepancies.

Though in this work we have concentrated on the channels and energies where there exists the largest set of spin-dependent data, the results arising from the 15CCO6 calculations include transitions from the ground state to any one of the states given in Table I, and may be obtained by electronic-mail. Also, upon request the 15CCO6 calculation may be performed at any other energy of interest to the reader.

ACKNOWLEDGMENTS

We would like to thank J. J. McClelland, M. H. Kelley, R. E. Scholten, G. F. Hanne, and D. H. Madison for the very many helpful communications and data transfers. We also acknowledge support from the Australian Research Council.

* Electronic address: igor@esm.cc.flinders.edu.au
† Electronic address: ian@esm.cc.flinders.edu.au

[1] J. J. McClelland, M. H. Kelley, and R. J. Celotta, Phys. Rev. A **40**, 2321 (1989).
[2] J. J. McClelland, S. R. Lorentz, R. E. Scholten, M. H. Kelley, and R. J. Celotta, Phys. Rev. A (to be published).
[3] R. E. Scholten, S. R. Lorentz, J. J. McClelland, M. H. Kelley, and R. J. Celotta, J. Phys. B **24**, L653 (1991).
[4] M. H. Kelley, J. J. McClelland, S. R. Lorentz, R. E. Scholten, and R. J. Celotta, in *Correlations and Polarization in Electronic and Atomic Collisions and (e,2e) Reactions*, edited by P. J. O. Teubner and E. Weigold (IOP, Bristol, England, 1992).
[5] S. R. Lorentz, R. E. Scholten, J. J. McClelland, M. H. Kelley, and R. J. Celotta, Phys. Rev. Lett. **67**, 3761 (1991).
[6] T. Hegemann, M. Oberste-Vorth, R. Vogts, and G. F. Hanne, Phys. Rev. Lett. **66**, 2968 (1991).
[7] H. L. Zhou, B. L. Whitten, G. Snitchler, and D. W. Norcross, Phys. Rev. A **42**, 3907 (1990).
[8] I. E. McCarthy and A. T. Stelbovics, Phys. Rev. A **28**, 2693 (1983).
[9] I. Bray, D. A. Konovalov, and I. E. McCarthy, Phys. Rev. A **43**, 5878 (1991).

[10] I. Bray, D. A. Konovalov, and I. E. McCarthy, Phys. Rev. A **44**, 5586 (1991).
[11] I. Bray, D. A. Konovalov, and I. E. McCarthy, Phys. Rev. A **44**, 7830 (1991).
[12] I. Bray, D. A. Konovalov, and I. E. McCarthy, Phys. Rev. A **44**, 7179 (1991).
[13] I. Bray, Phys. Rev. Lett. **69**, 1908 (1992).
[14] I. E. McCarthy, J. Mitroy, and R. Nicholson, J. Phys. B **24**, L449 (1991).
[15] L. V. Chernysheva, N. A. Cherepkov, and V. Radojevic, Comput. Phys. Commun. **11**, 57 (1976).
[16] L. V. Chernysheva, N. A. Cherepkov, and V. Radojevic, Comput. Phys. Commun. **18**, 87 (1979).
[17] C. E. Moore, *Atomic Energy Levels*, Natl. Bur. Stand. (U.S.) Circ. No. 467 (U.S. GPO, Washington, DC, 1949), Vol. 1.
[18] I. Bray, I. E. McCarthy, J. Mitroy, and K. Ratnavelu, Phys. Rev. A **39**, 4998 (1989).
[19] I. Bray and A. T. Stelbovics, Phys. Rev. A **46**, 6995 (1992).
[20] A. T. Stelbovics, Phys. Rev. A **41**, 2536 (1990).
[21] L. J. Allen, I. Bray, and I. E. McCarthy, Phys. Rev. A **37**, 49 (1988).
[22] D. H. Madison, K. Bartschat, and R. P. McEachran, J. Phys. B (to be published).
[23] G. F. Hanne (private communication).
[24] S. K. Srivastava and L. Vušković, J. Phys. B **13**, 2633 (1980).
[25] R. E. Scholten, P. J. O. Teubner, and G. F. Shen (unpublished).
[26] S. R. Lorentz and T. M. Miller (unpublished).